Cell. Mol. Life Sci. (2017) 74:67–83
DOI 10.1007/s00018-016-2389-5

Cellular and Molecular Life Sciences

MULTI-AUTHOR REVIEW

Architecture and functional properties of the CFTR channel pore

Paul Linsdell[1]

Received: 27 September 2016 / Accepted: 28 September 2016 / Published online: 3 October 2016

Abstract The main function of the cystic fibrosis transmembrane conductance regulator (CFTR) is as an ion channel for the movement of small anions across epithelial cell membranes. As an ion channel, CFTR must form a continuous pathway across the cell membrane—referred to as the channel pore—for the rapid electrodiffusional movement of ions. This review summarizes our current understanding of the architecture of the channel pore, as defined by electrophysiological analysis and molecular modeling studies. This includes consideration of the characteristic functional properties of the pore, definition of the overall shape of the entire extent of the pore, and discussion of how the molecular structure of distinct regions of the pore might control different facets of pore function. Comparisons are drawn with closely related proteins that are not ion channels, and also with structurally unrelated proteins with anion channel function. A simple model of pore function is also described.

Keywords ABC protein · CFTR · Channel pore · Chloride channel · Cystic fibrosis · Ion selectivity

Introduction

When the cystic fibrosis transmembrane conductance regulator (CFTR) was cloned in 1989, its function was not known [1]. Since CFTR is a member of the ATP-binding cassette (ABC) family of membrane transport proteins, most members of which function as ATP-dependent pumps of a broad range of different substrates [2–4], it seemed reasonable to assume that CFTR was also some kind of transport protein. We now know that, somewhat in spite of its ABC family heritage, CFTR functions as an ion channel that mediates the passive, electrodiffusional transport of Cl^-, HCO_3^- and other small anions across the cell membrane. To carry out this function, the CFTR protein must form a continuous aqueous pathway that allows these small ions to move rapidly between the intracellular and extracellular solutions. This pathway is referred to as the channel pore. Furthermore, in order for the transport of anions to be appropriately regulated, the channel pore must be able to interconvert rapidly between "open" and "closed" states that allow or prevent anion movement, respectively.

So far as we know, CFTR is the only ABC protein that has "ion channel" rather than "active transporter" as its primary job description [2, 3, 5]. As a result, the functional properties that define CFTR—rapid, passive movement of Cl^- and other small anions through an open channel pore—stand in contrast to its closest structural relatives in the ABC family. This contrast places strict limits on what we can learn about the molecular and biophysical bases of CFTR channel pore function from the study of other ABC proteins. On the other hand, other anion channel families that are known at the molecular level—including ligand-gated anion channels [6–8], ClC channels [9], TMEM16 (anoctamin) channels [10], bestrophins [11] and LRRC8 [12]—show no apparent structural homology to CFTR, and so again can offer us little assistance in understanding the molecular basis of CFTR's anion channel function. This review summarizes what is presently known about how CFTR transports Cl^- and other small anions across the cell membrane. Current understanding of the molecular basis of anion transport—the molecular architecture of the pathway

✉ Paul Linsdell
paul.linsdell@dal.ca

[1] Department of Physiology and Biophysics, Dalhousie University, PO Box 15000, Halifax, NS B3H 4R2, Canada

taken by Cl^- ions to cross the membrane via CFTR—is described. This includes a review of studies investigating the structural underpinnings of the observed functional properties of CFTR-mediated Cl^- transport, and what this might tell us about the molecular mechanism of anion permeation. Implications for the structural relationship between CFTR and its active transporter ABC relatives, as well as the functional relationship between CFTR and structurally unrelated anion channel types, are also discussed.

Functional properties of the channel pore

The physiological role of CFTR is as a regulated anion conductance in the apical membrane of many different epithelial cell types [13]. As will be described in detail below, the membrane-spanning parts of the CFTR protein directly form the transmembrane pore for the transport of Cl^- and other small anions. The opening and closing of this channel pore is controlled by ATP binding and hydrolysis by the cytoplasmic nucleotide binding domains (NBDs) [5, 14]. Physiological regulation of channel activity is predominantly via cyclic AMP/protein kinase A (PKA) signaling [13], with PKA-dependent phosphorylation of the CFTR protein being required for channel activity [15, 16].

Functional properties of the CFTR pore have been characterized using biophysical approaches. At the single channel level, CFTR has a linear current–voltage relationship with a slope conductance of ~6–9 pS (Fig. 1a, b). In spite of this linearity and a lack of voltage-dependence in channel activity, the macroscopic current–voltage relationship in intact cells often exhibits mild outward rectification (see below). The measured single-channel conductance shows a saturating dependence on Cl^- concentration, suggesting an overall Cl^- affinity for the pore of around 55 mM (Fig. 1c).

In addition to Cl^-, many other anions are able to permeate through the CFTR channel pore. As with most anion channels, the ability of CFTR to discriminate between different anions—referred to as the selectivity of the channel—is low, especially when compared to the highly selective K^+, Na^+ and Ca^{2+} channels. Selectivity of ion channels can be represented in different ways, two of the more commonly expressed of which are (1) the relative permeability of different ions (which reports the relative likelihood a type of ion will be transported), and (2) the relative conductance of different ions (which reports the relative rate at which different ions pass through the channel).

The relative permeability of different monovalent anions in CFTR decreases as a function of anion size (Fig. 1d). This has been used to estimate that the narrowest part of the open channel pore must have a diameter of ~5.3 Å; anions with dimensions larger than this cut-off size cannot pass through the channel [17]. It should be stressed that this "narrowest part" may extend over a very short section of the pore, and that other parts of the pore may be significantly wider. It is also important to remember that this value represents a functional diameter with no direct physical meaning. Among small monovalent anions, the usually reported sequence of permeability ratios in CFTR is [16–18]:

$$SCN^- > NO_3^- > Br^- > Cl^- > I^- > \text{formate} > F^-$$

It has been noted that this sequence suggests a relationship between anion permeability and anion hydration energy [19–22] (Fig. 1e). This relationship reflects a "lyotropic" or weak field strength sequence, with weakly hydrated anions (lyotropes like SCN^-) tending to show a higher permeability than anions that bind water molecules more strongly (kosmotropes like F^-) (Fig. 1e). The observed

Fig. 1 Functional properties of the CFTR channel pore. **a** Example single channel currents recorded under symmetrical high [Cl^-] conditions at membrane potentials of +50 mV (*top*) and −50 mV (*bottom*). In each case the closed state current is indicated by the *line to the left*. **b** Mean single channel current–voltage relationship under these conditions. The *straight-line* fit indicates a slope conductance of 8.1 pS. These two panels show unpublished data from the author's laboratory, under conditions reported recently [27, 51, 91]. **c** Relationship between single channel conductance (γ) and Cl^- activity (under symmetrical ionic conditions). Fit to a Michaelis–Menten-type hyperbolic function suggests a maximal saturating conductance of 11.1 pS and an affinity of the channel for Cl^- ions of 53.9 mM. Re-plotted using data from, and fitting procedure described in, Ref. [84]. **d** Relationship between anion relative permeability and anion diameter, both for lyotropic (*open symbols*) and kosmotropic anions (*filled symbols*). Fits to both data sets suggest a minimal pore diameter of 5.3 Å. Anions shown are (*left to right*): *open symbols* SCN^-, Cl^-, NO_3^-, Br^-, I^-, ClO_4^-, benzoate, PF_6^-; *closed symbols* formate, acetate, propanoate, pyruvate, methane sulfonate, gluconate. Re-plotted using data from, and fitting procedure described in, Ref. [17]. **e** Relationship between anion permeability and anion hydration energy for selected small anions. Re-plotted using data from [21]. **f** Relationship between anion permeability and anion hydration energy for selected small anions. Re-plotted using data from [23]. **g** Voltage-dependent block of macroscopic current by cytoplasmic 5-nitro-2-(3-phenylpropylamino)benzoic acid (NPPB; 30 μM). Unpublished data under conditions similar to those described previously [46, 63]. **h** Voltage-dependent block of macroscopic current by cytoplasmic $Au(CN)_2^-$ ions (100 μM). Re-plotted using data from [102]. **i** Macroscopic current–voltage relationships recorded before (on-cell) and after (inside-out) excision of the patch from the cell. The increase in current amplitude when the patch is excised from the cell, in particular at negative voltages, is thought to reflect relief from voltage-dependent block by unknown cytoplasmic anions [63, 73]. Re-plotted using data from [63]. **j** Block of single-channel current by cytoplasmic NPPB (10 μM) at a membrane potential of −40 mV, under different ionic conditions from those shown in **g** (low (4 mM) external Cl^- concentration) (unpublished data). As originally described by Zhang et al. [105], NPPB causes repetitive flickery blocking events characteristic of a kinetically intermediate blocking reaction. **k** Block of single-channel current by cytoplasmic $Au(CN)_2^-$ ions (100 μM) at a membrane potential of −60 mV, under the same ionic conditions as shown in **h**. Re-plotted using data from [102]

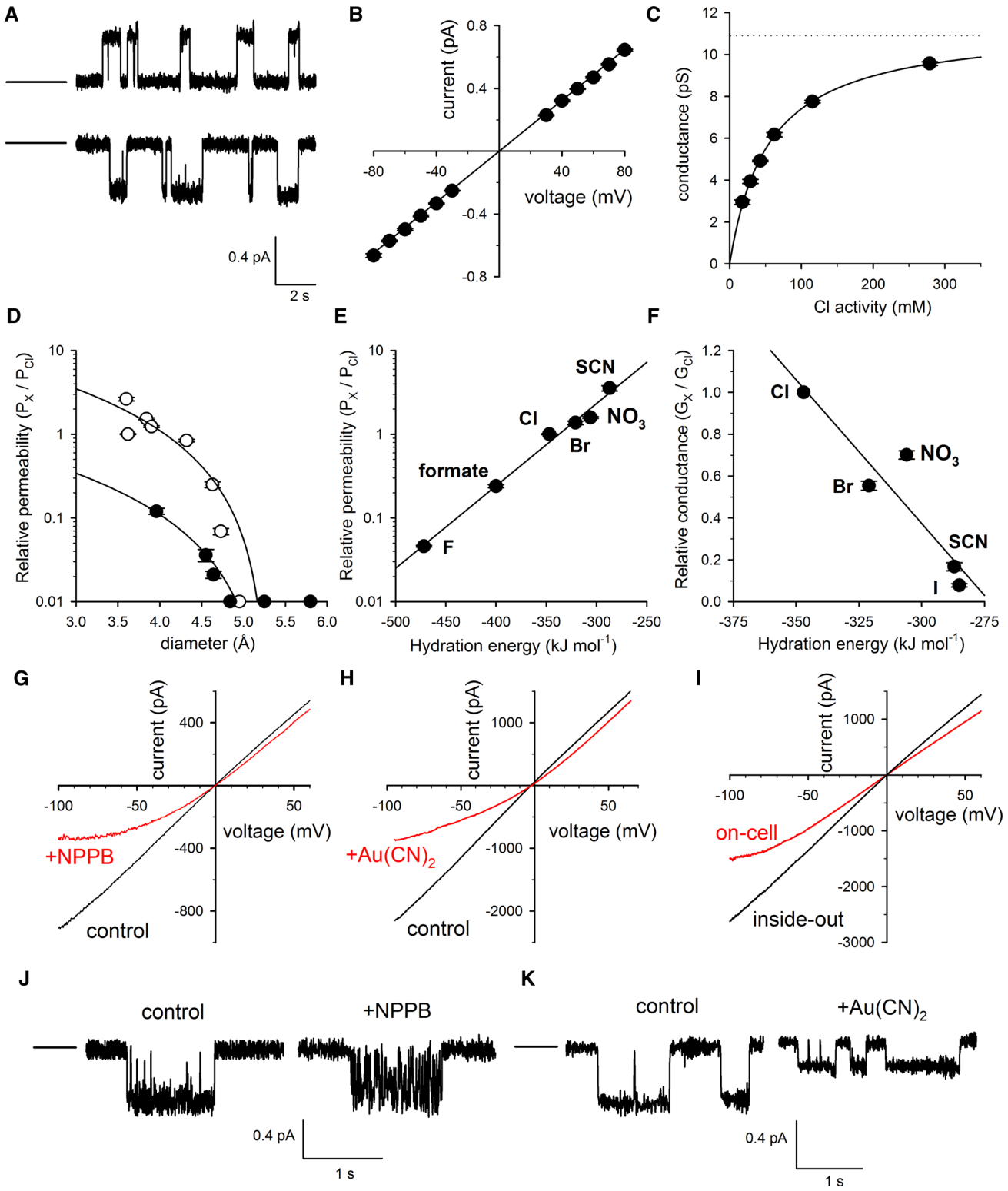

lyotropic relationship between permeability and hydration energy has been used to suggest that anion dehydration is a limiting step in the anion permeation process, as anion:water interactions are replaced by energetically favourable interactions between the anion and amino acid groups lining the pore [20–22].

The relative conductance of different anions is more difficult to quantify experimentally [23], however, under

the most unambiguous conditions the sequence of conductance ratios has been reported as [23, 24]:

$$Cl^- > NO_3^- > Br^- \sim \text{formate} > SCN^- > I^-$$

Among small lyotropic anions with relatively high permeability, anion conductance also appears to be strongly correlated with anion hydration energy (Fig. 1f): lyotropic anions that are more easily dehydrated show lower conductance.

The channel pore also has the capacity to bind anions. This is most readily apparent from the effects of anions that bind tightly enough within the pore to temporarily occlude the permeation pathway, blocking the passage of Cl^- ions. Many such open channel blocking anions have been shown to act from the cytoplasmic side of the membrane [25]. This includes large organic anions that are too large to pass through the channel [25] (Fig. 1g) as well as highly permeant, strongly lyotropic anions [20, 24, 26] (Fig. 1h). The ability of highly lyotropic anions such as $Au(CN)_2^-$ and SCN^- to block Cl^- permeation through the open channel has been used to suggest that the relative strength of anion binding within the pore is also dependent on anion hydration energy [20, 24]; a recent study suggested that anion binding affinity follows the sequence [23]:

$$SCN^- \sim I^- > Br^- > NO_3^- > Cl^- \geq \text{formate}$$

Again, this sequence is consistent with anion binding strength following a lyotropic sequence (more lyotropic anions bind more tightly). Intracellular open-channel blocking anions usually show voltage-dependent effects on Cl^- permeation, with block being stronger at more hyperpolarized voltages that favour entry of negatively charged substances into the pore from its cytoplasmic end (Fig. 1g, h). This voltage-dependence suggests that the blocking anion crosses part of the transmembrane electric field as it passes between the cytoplasm and its binding site inside the channel pore [25]. Furthermore, block by these substances is sensitive to the extracellular Cl^- concentration, being stronger at low Cl^- and weaker at higher Cl^- [25, 27]. This Cl^--sensitivity is usually ascribed to repulsive interactions between Cl^- and blocking anions that occur when both are bound inside the pore at the same time [25, 27]. Depending on the duration of the blocker binding event, the blocker may cause brief, discrete interruptions of single-channel current (indicative of a kinetically "intermediate" blocking reaction) (Fig. 1j), or it may cause an apparent decrease in unitary current amplitude when individual blocking events are unresolved (indicative of a kinetically "fast" blocking reaction) (Fig. 1k) (for a recent review, see [25]). Many different organic anions have been shown to block the channel exclusively or preferentially from its cytoplasmic side, suggesting the presence of an anion binding site that is relatively easily accessible from the cytoplasm and which shows little specificity between anions [25]. In fact, the property of outward rectification of the CFTR current–voltage relationship often observed in intact cells appears to be the result of voltage-dependent channel block by unknown cytoplasmic anions [25] (Fig. 1i). In addition to this seemingly non-specific blocking effect of cytoplasmic anions, some anions may be able to block the channel pore from the extracellular side [28–30], perhaps indicating the existence of externally accessible binding site(s) in the pore.

It has been noted previously that many of these functional characteristics of the CFTR channel pore are similar to those of other anion channel types that, as described above, are not structurally related to CFTR. Common functional properties such as high permeability of lyotropic anions, low conductance of lyotropic anions, tight binding of highly lyotropic permeant anions such as SCN^-, and overlapping blocker sensitivity (in particular to relatively hydrophobic organic anions) occur in most anion channel types that have been studied in detail [20, 31–36]. The extent to which this functional overlap reflects similarities in overall pore architecture and/or in the molecular mechanism of anion permeation and selectivity must await more complete characterization of the structures, and the anion permeation mechanisms, of diverse anion channel pores.

Structure of the pore

At the time of writing, a high-resolution structure of the membrane-spanning parts of CFTR has not been published. As such, the actual structure of the pore is not currently known. It is presumed that the overall architecture of CFTR is similar to that of closely related ABC proteins [37, 38]. As with other ABC proteins, CFTR has a modular architecture consisting of two membrane-spanning domains (MSDs)—each composed of six membrane spanning α-helices (TMs)—and two cytoplasmic NBDs (Fig. 2a). Connecting the two pseudosymmetrical MSD-NBD "halves" of the protein is a cytoplasmic regulatory domain that is not found in any other ABC protein (Fig. 2a). Individual TMs are connected at their extracellular ends by short extracellular loops (ECLs) and at their cytoplasmic ends by long intracellular loops (ICLs); these ICLs are now thought to form extensions of the TM α-helices into the cytoplasm (Fig. 2a–c). High resolution structures for several CFTR-like ABC proteins are available [4, 39–41], and some of these have been used as templates to produce atomic homology models of CFTR. For example, Fig. 2 shows two recently published models

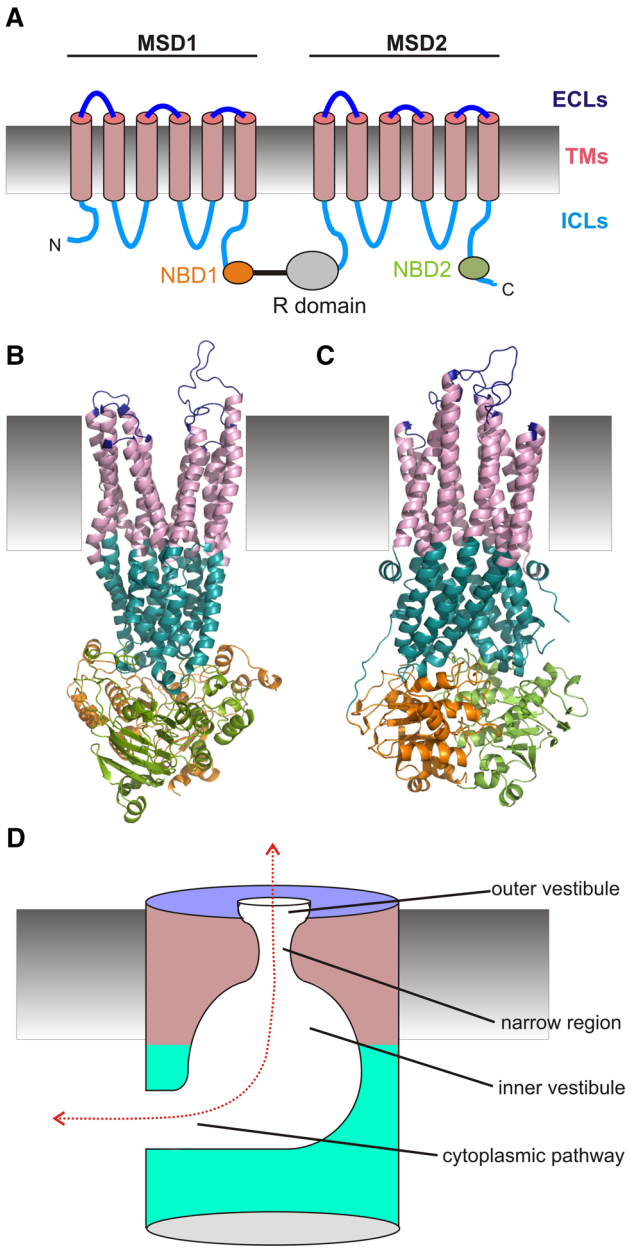

Fig. 2 Models of the CFTR pore. **a** Overall two-dimensional topology. The protein is comprised of two MSDs, each made up of six TMs (*magenta*) connected by short ECLs (*blue*) and longer ICLs (*cyan*). Each MSD is followed by a cytoplasmic NBD (NBD1 *orange*, NBD2 *green*). The two MSD:NBD repeats are connected by the cytoplasmic regulatory (R) domain (*grey*). Recent atomic homology models of CFTR in the putative open state, based on bacterial transporters Sav1866 (**b**) [42] and McjD (**c**) [43]. *Same colour* scheme as in **a** to represent the approximate extent of the ECLs, TMs, ICLs and NBDs. Note that the R domain is absent from both of these two models. **d** Cartoon model of the pore, based on functional investigation. As described in the text, the pore has a narrow region near its outer end, flanked by wider outer and inner vestibules. The inner vestibule is connected to the cytoplasm by a cytoplasmic pathway with an entrance via at least one lateral portal. *Same colour* scheme as in **a**–**c** to indicate that the ECLs, TMs and ICLs all contribute to different parts of the pore

described as depicting CFTR in the putative open state, one based on the bacterial multidrug exporter Sav1866 [42] (Fig. 2b) and one based on the bacterial peptide transporter McjD [43] (Fig. 2c). However, because the membrane-spanning parts of these proteins are the region not only of lowest sequence identity with CFTR, but also presumably the lowest functional similarity (since these templates are active transport proteins of large substrates and CFTR is a Cl^- channel; and since active transporter proteins, by definition, lack a continuously open substrate transport pathway as in an open ion channel), the suitability of these models to describe the structure of the channel pore of CFTR has been criticized [22]. On the other hand, since CFTR shows no structural similarity to other kinds of anion channels, these ABC protein-derived models must represent the closest structural models currently available for CFTR.

The overall topology of the CFTR channel pore has been inferred from functional analysis using electrophysiological approaches (Fig. 2d). As described above, the narrowest part of the pore has been estimated to have a functional diameter of ~5.3 Å (Fig. 1d). Because organic anions with dimensions that are very much larger than this are able to enter into the pore from the cytoplasm to cause voltage-dependent channel block, it was proposed that the narrow region is connected to the cytoplasm by a wide "inner vestibule" within which large anions can bind [25, 44–46]. Because in many cases these large blocking anions are ineffective when applied to the extracellular side of the membrane, any "outer vestibule" connecting the narrow region to the extracellular solution might be expected to have more restricted dimensions (Fig. 2d). Recently, both homology modeling [42, 43] and structure–function analysis [47, 48] have been used to suggest that the inner vestibule is connected to the cytoplasm not by a centrally located route, but instead via a "lateral portal" formed by the long ICLs that form cytoplasmic extensions of individual TMs (Fig. 2b–d). As will be discussed, traditional structure–function analysis, as well as substituted cysteine accessibility mutagenesis (SCAM) analysis of the TMs and ICLs, has now allowed us to begin to understand the molecular bases of these different parts of the pore, as well as giving some insight into how interactions between anions and amino acid side-chains lining these different pore regions govern the functional properties of the channel.

It should be stressed that the functional model shown in Fig. 2 is based on experimental investigation of ionic current passing through the CFTR channel while it is open, and is therefore, proposed to represent the open state of the pore. The structure and function of the pore when it is closed is, of course, more difficult to characterize using

traditional electrophysiological assays. However, characterizing the differences in pore structure between open and closed states is important if we are to understand the conformational change(s) that underlie the channel opening and closing process. The structure of the closed channel pore has been probed using substances that can interact with the pore while it is closed, including cysteine-modifying reagents [49], metal ions [50] and pore-blocking anions [51]. Possible changes in pore architecture associated with channel opening and closing will be described only briefly in this review.

Shape of the permeation pathway

Amino acid residues lining the anion permeation pathway have been identified using SCAM (Fig. 3). To date, the entire lengths of TM6 [52, 53] and TM12 [54, 55] have been shown to line the pore, as well as more restricted parts of TM1 [56, 57] and TM11 [58, 59] and the extreme internal and external ends of TM5 [60] (Fig. 3a–c). While CFTR's two internal repeats are expected to result in a symmetrical arrangement of TMs (Fig. 3c), it has been noted that the identities of the main pore-forming TMs (TMs 1, 6, 11, 12) suggest an asymmetric pore [59], perhaps being formed slightly off-centre from the central axis of the MSDs (Fig. 3c). Furthermore, while symmetrically located TMs 6 and 12 both contribute to the entire length of the TM pore [52–55], it has long been recognized that these two TMs play very different roles in determining pore functional properties [61], which appear to be dominated by amino acid residues in TM6 [59, 62].

More recently, amino acid residues in the cytoplasmic extensions to TMs 3, 4, 5 and 6 have been shown to line the permeation pathway, likely contributing to the lateral pathway that connects the cytoplasm to the transmembrane pore [47, 48] (Fig. 3a–c). Again, the apparently dominant role played by the lateral portal in funneling cytoplasmic Cl^- ions to the pore suggests a highly asymmetric structure to the Cl^- permeation pathway, with Cl^- ions entering this pathway from one "side" rather than centrally [47, 48] (Fig. 3c).

Throughout the TMs and their cytoplasmic extensions are positively charged arginine and lysine side chains that have been shown to attract Cl^- ions and contribute to the maximization of channel conductance. Neutralization of the positive charge at K95 (TM1) [62, 63], R104 (TM1) [30], K190 (extension to TM3) [47], R248 (extension to TM4) [47], R303 (extension to TM5) [64], R334 (TM6) [29, 65], K335 (TM6) [30, 65], R352 (TM6) [64], K370 (extension to TM6) [47], K1041 (extension to TM10) [47] and R1048 (extension to TM10) [47] has been shown to reduce Cl^- conductance, consistent with a role for the native positive charge in electrostatic interactions with permeating Cl^- ions. The locations of these important positive charges within different representations of the channel are illustrated in Fig. 3d–f. Functionally important positive charges are found in the outer vestibule, inner vestibule and cytoplasmic pathway (Fig. 3e), and when viewed from the side appear quite evenly spread throughout the permeation pathway, with no obvious large gaps between neighbouring charged residues (Fig. 3e). In contrast, when viewed from above, it is clear that these positive charges are clustered along one side of the pore (Fig. 3f), adding to evidence that the pore exhibits a highly asymmetric organization. If, as electrostatics would suggest, Cl^- ions follow the trail of positively charged side-chains lining the pore, then the putative location of these charges illustrated in Fig. 3f would suggest that Cl^- ions enter from the cytoplasm via a lateral portal between the ICLs [42, 43, 47, 48] and then pass along a pathway well off-centre through the TMs. How the highly asymmetric location of key pore-lining positive charges shown in Fig. 3f relates to the overall asymmetric contribution of different TMs to the permeation pathway shown in Fig. 3c is not currently clear.

Structural basis of channel function

The function of the CFTR pore is to form a pathway via which Cl^- and other small anions may cross the membrane rapidly by an electrodiffusional mechanism. The overall shape of this pathway, as defined by SCAM, is described in the preceding paragraphs and summarized in Fig. 3. The following sections will review the evidence for the ways in which the functional properties of the channel pore are determined, as characterized using structure–function analysis. For simplicity's sake, I will divide the pore into different regions along the lines defined in Fig. 2d—outer vestibule, narrow region, inner vestibule, and cytoplasmic pathway—and deal with these regions one at a time (see Fig. 4), notwithstanding the fact that the boundaries between these functional regions are indistinct and would likely be placed in slightly different locations (if at all) by different authors.

Anion attraction by the outer vestibule

The TMs are connected by short ECLs, such that very little of the protein is exposed to the extracellular solution (Fig. 2b, c). There is some evidence from SCAM and cysteine cross-linking studies that specific residues within the ECLs are exposed to the extracellular solution [66, 67], and it has been suggested that the ECLs may be involved in the regulation of channel gating [66–69]. Furthermore, at

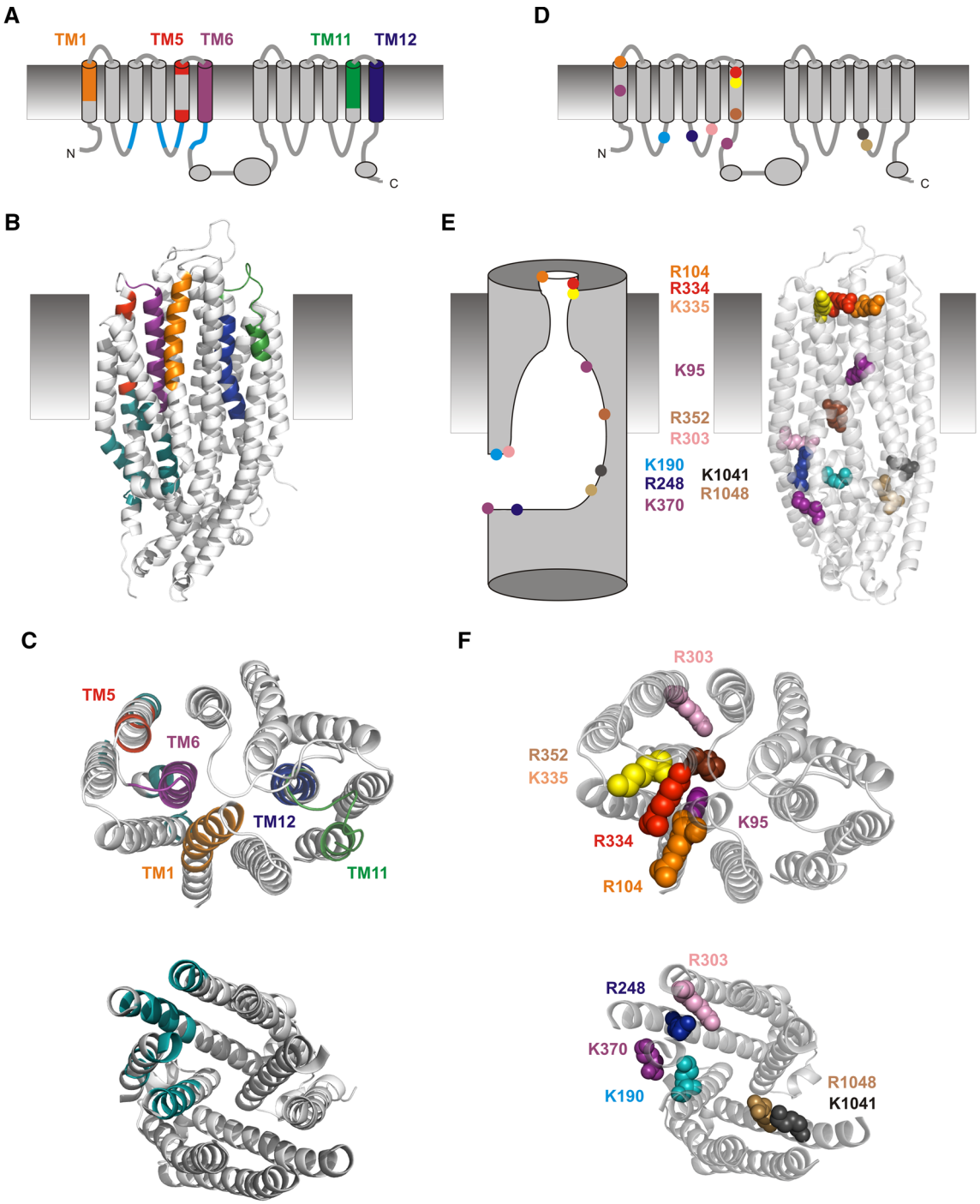

Fig. 3 Overall shape of the CFTR pore. Different TMs and ICLs contributing to the permeation pathway, as defined by SCAM and functional investigations described in the text. The same information is presented in terms of overall cartoon topology (**a**) and in one recent atomic homology model of CFTR based on McjD [43], viewed from the side (**b**) and from above (**c** TMs *top*, ICLs *below*). For clarity, the NBDs have been removed in these models. The transmembrane pore (outer vestibule, narrow region, inner vestibule) is lined by parts of TMs 1 (*orange*), 5 (*red*), 6 (*purple*), 11 (*green*) and 12 (*blue*). The cytoplasmic pathway is formed by cytoplasmic extensions to TMs 3, 4, 5 and 6 (*cyan*). **d–f** Location of functionally important positively charged arginine and lysine residues that have been proposed to interact with permeating Cl^- ions. The approximate locations of these charged residues is represented both in cartoon form (**d**, **e**) and in the same atomic model representations as in **b**, **c** reproduced in **e**, **f**. Within this model, selected positively charged side-chains are shown as space-filling models. Positively charged residues indicated in **d–f** are as follows: K95 (TM1) *purple*; R104 (TM1) *orange*; K190 (cytoplasmic extension to TM3) *cyan*; R248 (extension to TM4) *blue*; R303 (extension to TM5) *pink*; R334 (TM6) *red*; K335 (TM6) *yellow*; R352 (TM6) *brown*; K370 (extension to TM6) *purple*; K1041 (extension to TM10) *grey*; and R1048 (extension to TM10) *gold*

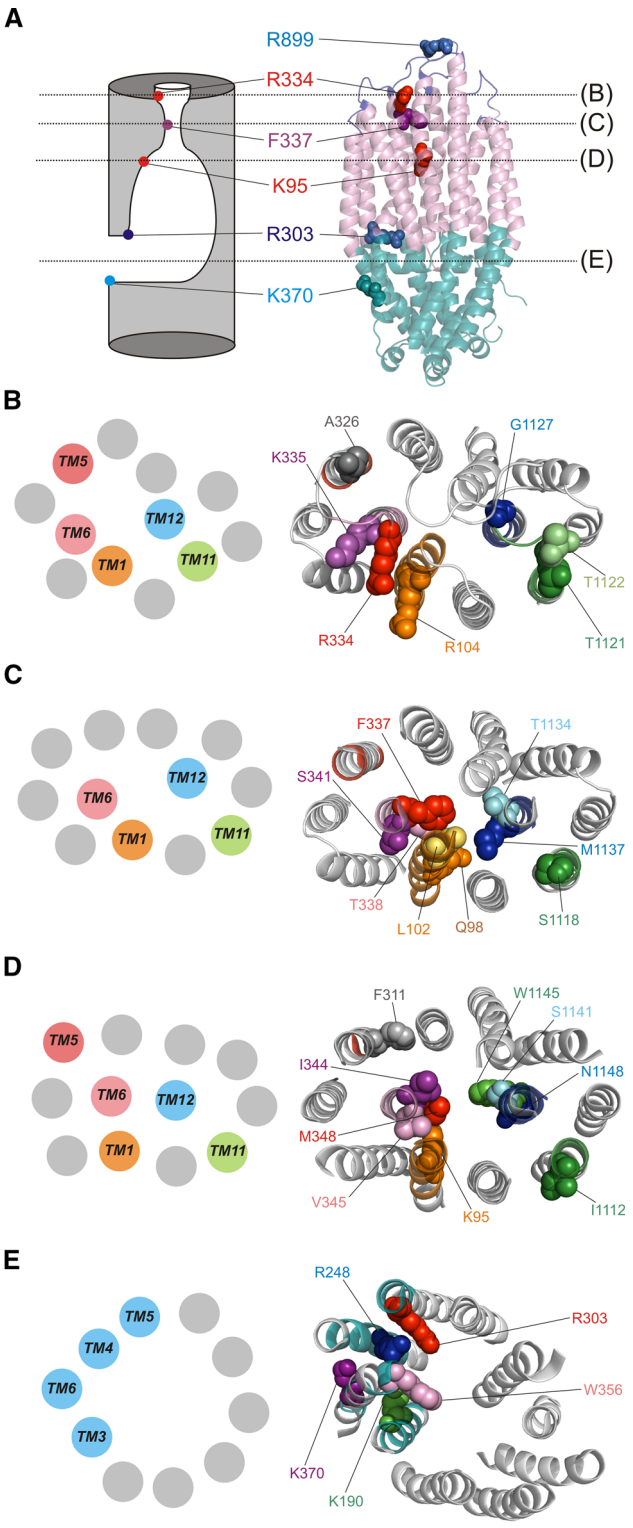

◀**Fig. 4** Amino acid side-chains determining the functional properties of different regions of the CFTR pore. **a** Approximate locations of different regions of the pore, in cartoon form (*left*) or in the atomic homology model representation used in Fig. 3 (*right*) and *coloured* according to Fig. 2 (ECLs *blue*, TMs *magenta*, ICLs *cyan*). The putative location of several key residues is indicated in both models for orientation. *Dashed lines* labeled **b**–**e** show the approximate levels of "slices" through the channel used to illustrate the proposed structure of different regions of the pore in corresponding panels (**b**–**e**), which are shown from above. **b** The outer vestibule is lined by TMs 1, 5, 6, 11 and 12. **c** The narrow region is lined by TMs 1, 6, 11, and perhaps 12. **d** The inner vestibule is lined by TMs 1, 5, 6, 11 and 12. **e** The cytoplasmic pathway is lined by the cytoplasmic extensions to TMs 3, 4, 5 and 6. Some selected key amino acid side-chains mentioned in the text are shown as space-filling models in **b**–**e**

least one ECL residue [R899 in ECL4 (Fig. 4a)] has been proposed to interact with extracellular anions [70, 71], perhaps allowing channel function to be regulated by the anion composition of the extracellular fluid [72, 73]. However, it appears that the ECLs make little or no functional contribution to the Cl^- permeation pathway [70, 74].

At the outer mouth of the pore itself, Cl^- ions are likely attracted by positively charged amino acid side-chains R104 (TM1), R334 (TM6) and K335 (TM6) (Fig. 3d–f). SCAM evidence confirms that these and other side-chains at the outer ends of TM1 [30, 57], TM5 [60], TM6 [65, 75], TM11 [58] and TM12 [58] are accessible to extracellular water-soluble cysteine-reactive methanethiosulfonate (MTS) reagents, and therefore, presumably relatively accessible from the extracellular solution (Fig. 4a, b).

Mutations that neutralize the positive charges at R104, R334 and K335 have several effects in common: causing reduced single channel conductance, inducing outward rectification of the current–voltage relationship (indicating a larger effect on anion influx than on anion efflux), and weakening the blocking effects of extracellular pore-blocking $Pt(NO_2)_4^{2-}$ ions [29, 30, 65]. This has led to the suggestion that each of these positive charges acts to attract Cl^- ions electrostatically from the extracellular solution to the pore [30, 65]. However, there are also important differences in the effects of mutations at these positions that potentially point to different functional roles. At both R104 and K335, mutation to neutral or negatively charged side-chains—as well as modification by positively or negatively charged MTS reagents following mutation to cysteine—have been used to demonstrate strictly charge-dependent effects on conductance and current–voltage rectification [30, 65], consistent with an electrostatic role of these charges in interacting with permeating Cl^- ions. The effects of different mutations and MTS modifications at R334 are somewhat more complex, however. All mutations studied at R334—including the charge-conservative R334K—greatly reduce single channel conductance [76], inconsistent with a purely electrostatic effect. Similarly, the reduced conductance of R334C can be only partly restored following modification by a positively charged MTS

reagent [65]. Effects on macroscopic current–voltage relationship rectification, however, do show a strict relationship with predicted side-chain charge at position 334 [46, 65, 77], suggesting that R334 may have both charge-dependent and charge-independent effects on Cl^- permeation. Channel block by extracellular $Pt(NO_2)_4^{2-}$ ions appears to require a positive charge at position 334 [29], also supporting an electrostatic interaction with extracellular anions. Mutations at position R334 have also been shown to have charge-independent effects on interactions between the pore and intracellular anions [29, 77], which has been used to suggest that mutation of the native arginine at this site causes long-range changes in the conformation of the protein that disrupt inner vestibule function [29]. It has also been suggested that R334 forms a state-dependent salt bridge with E217 in ECL2 [78], potentially allowing R334 to exert a broad influence over the conformation of the outer vestibule. In summary, while R104, R334 and K335 each appear to play a role in electrostatic attraction of Cl^- ions necessary for optimal Cl^- conductance, mutation of R334 also appears to have other effects that cannot be explained by a direct electrostatic interaction with permeating anions and that may instead point to additional role(s) of this residue in the control of channel structure and function.

Uncharged amino acid side-chains also contribute to the outer vestibule (Fig. 4b). At the extracellular end of TM1, mutations I106C and A107C slightly reduce single channel conductance, and these introduced cysteines are also accessible to extracellular MTS reagents [57]. Cysteines substituted for TM5 residues L323 and A326 are also accessible to extracellular MTS reagents [60]. Several residues in ECL6, joining the extracellular ends of TM11 and TM12, are accessible to extracellular, but not intracellular, MTS reagents [49, 58], namely T1121, T1122, G1127, V1129, I1131 and I1132. Cysteine substitution for T1121, T1122 and G1127 slightly reduces conductance at positive membrane potentials, indicating some functional role in Cl^- permeation [58]. Furthermore, MTS modification at each of these six positions in TMs 11–12 has charge-dependent effects on Cl^- conductance at positive membrane potentials, consistent with charge deposition within the outer vestibule having an electrostatic effect on the attraction of Cl^- ions from the extracellular solution [58].

Functional investigation has also provided some information on the three-dimensional structure of the outer vestibule. The formation of disulfide bonds between introduced cysteine side-chains has been used to suggest a physical proximity between R334 and both T1122 and G1127 [79]. The propensity of these disulfide bonds to form in open channels and in closed channels was used to suggest that R334 is closer to T1122 when the channel is open, and closer to G1127 when the channel is closed [79]. For these disulfide bonds to form, it is generally considered that the S–S distance between the two cysteine side-chains must be $\sim$2 Å, with the Cβ-Cβ distance $\sim$3.4–4.6 Å and the Cα-Cα distance $\sim$3.8–6.8 Å [80], placing important constraints on the three-dimensional structure of this part of the pore (Fig. 4b).

Several studies have suggested that the structure of the outer vestibule changes during channel gating. As described above, it has been suggested that R334 and E217 form a salt bridge in closed channels, and that this salt bridge breaks when the channel opens as TM6 and ECL2 move apart [78]. Also as described above, changes in the proximity of R334, T1122 and G1127 in open channels and in closed channels has been used to suggest a relative translational movement of the outer parts of TM6 and TM11 during channel gating [79]. It has also been noted that, somewhat surprisingly, the accessibility of cysteine substituted for both R334 [81, 82] and K335 [75, 83] to extracellular substances is reduced in open channels compared to closed channels. This has been used to suggest that the outer vestibule is wide open to the extracellular solution when the channel is closed, and that it actually constricts somewhat during channel opening [82].

Anion selectivity at the narrow region

As described above (see "Functional properties of the channel pore"), the narrowest part of the channel pore has a functional diameter of $\sim$5.3 Å, based on the dimensions of permeant and impermeant anions (Fig. 1d). Early experiments investigating the permeability of organic anions with dimensions close to this cut-off size suggested that the narrow size-selectivity filter might be located close to TM6 residues T338 and T339 [84]. This approximate location of the narrow region (Fig. 4a, c) is now supported by evidence for the furthest extent of large MTS reagent penetration into the pore from either end [49], by current molecular models of the pore [42, 43], and by functional effects of mutations in this region, in particular at TM6 residues F337, T338 and S341 (as described in detail below). SCAM evidence suggests that, in addition to TM6 [52, 53, 75], TM1 [30, 57] and TM11 [59] line the narrow region of the pore (Fig. 4c).

The narrow region—and more specifically, that part of TM6 that contributes to this region—appears to play a dominant role in defining the permeability selectivity of the channel between different anions. This very fact is consistent with the existence of relatively narrow ion "selectivity filters" in other ion channel types, in which relatively close interactions between permeating ions and the pore walls determine ion selectivity [85, 86]. Among CFTR mutations that have been investigated, those at

F337, T338 and S341 have almost unique powers to alter the relative permeabilities of different anions. In terms of altering the normal lyotropic sequence of anion permeabilities (Fig. 1e), mutations that decrease the side-chain volume at position F337 have the most significant effects. Thus, the mutations F337A and F337S result in a channel with a greatly reduced ability to select for different anions based on their energy of hydration (Fig. 1e), with reduced permeability of lyotropic anions, increased permeability of kosmotropic anions, greatly diminished discrimination between lyotropic and kosmotropic anions, and a significantly altered anion permeability selectivity sequence [21]. Other mutations substituting larger side-chains (F337L, F337W, F337Y) have much less effect on anion selectivity and similar permeability sequences as wild-type, suggesting that it is the size of the amino acid side-chain at this position that is the factor predominantly determining lyotropic anion permeability selectivity [21].

Mutations at the adjacent TM6 residue, T338, also disrupt the normal anion permeability sequence, although their effects are somewhat different to mutations at F337. Several different substitutions at this position were found to alter the selectivity sequence without changing the overall preference for lyotropic over kosmotropic anions; in fact, in most cases the relative permeability of highly lyotropic anions such as SCN^-, NO_3^- and ClO_4^- was significantly increased relative to wild-type [87]. As such, it could be considered that mutations at this site have a qualitatively "opposite" effect on anion selectivity to F337A and F337S described above: mutations at T338 tend to enhance the normal lyotropic nature of anion selectivity [87], whereas F337A and F337S disrupt lyotropic selectivity [21]. Substituting a small amino acid side-chain (T338A) also led to a significant increase in the permeability of organic anions, the permeability of which is likely limited by steric factors at the narrow region of the pore (Fig. 1d), hinting that the T338A mutation widens the narrow region; however, substituting a larger side chain (e.g. T338V) did not result in a decrease in organic anion permeability that might suggest a narrower-bore pore [87]. Mutations at S341, closer to the intracellular end of the narrow region, significantly alter the relative permeability of different anions without changing the overall anion selectivity sequence [18, 88], suggesting a more moderate impact on the anion selectivity process. In contrast, mutation of amino acids from other TMs that are purported to be close to the narrow region—for example Q98 (TM1) [62], S1118 (TM11) [59], T1134 (TM12) [18, 61] and M1137 (TM12) [61]—had negligible effects on anion permeability ratios.

Mutations close to the narrow region—both in TM6 and in other TMs—have been shown to have strong effects on Cl^- conductance. Mutations at F337 (F337A, F337S) [24] and S341 (S341A, S341K) [63, 89] greatly reduce conductance (to <25 % of wild-type conductance). At T338, mutations have strongly size-dependent effects on conductance; while substitutions of larger side-chains (T338I, N, V) reduced conductance by >90 %, below the resolution limit of single channel recording, smaller substitutions (T338A, T338S) actually increased conductance by >30 % [87]. This strongly size-dependent effect on conductance is consistent with the T338 side-chain existing in a physically restricted region of the pore where amino acid side-chain volume directly impacts Cl^- permeation. Since the T338A mutation also allows increased movement of pore-blocking $Au(CN)_2^-$ ions between different sites in the pore, it has been suggested that T338 contributes to a barrier within the pore that limits the rate of ion permeation [90]. Beyond TM6, mutation of TM1 residues Q98 [57, 62, 91] and P99 [57, 62, 92] greatly reduce conductance. Smaller, but significant, effects on conductance have also been reported following mutation of L102 (TM1) [57], S1118 (TM11) [58, 59] and T1134 (TM12) [89, 93].

There is little functional evidence relating to the three-dimensional structure of the narrow region (Fig. 4c). Cysteines substituted for T338 and S1118 are able to form a disulfide bond, and it was suggested that this bond forms preferentially in the channel open state, suggesting that these two side-chains are in close proximity in open channels [79]. Perhaps consistent with this idea, mutations that reduce side-chain volume at these two positions have somewhat additive effects on anion selectivity and $Au(CN)_2^-$ block, although not on single channel conductance [59]. Metal bridges formed by Cd^{2+} ions coordinated by two cysteine side-chains have also been used to demonstrate close proximity between T338 and S1118 [79], as well as between L102 and S341 [94]. These metal bridges are thought to form when the S–S distance between coordinating cysteine side-chains is $\sim$5 Å [80].

In addition to its well-established roles in the control of anion selectivity and Cl^- conductance, it has recently been suggested that the narrow region of the pore forms the "gate" that controls channel opening and closing [43, 83, 95]. In particular, it has been suggested that the large, hydrophobic F337 side-chain might occlude the Cl^- permeation pathway in the closed state, and then move to allow Cl^- permeation in the open state [43, 95].

Anion binding in the inner vestibule

The inner vestibule of the pore was initially described as a relatively wide region of the pore where large organic channel blockers entering from the cytoplasmic solution could bind to occlude the pore and physically prevent the passage of Cl^- ions [25, 44–46]. Consistent with this inner vestibule being readily accessible to the cytoplasmic

solution, SCAM investigation has shown that large MTS reagents can enter the pore from its cytoplasmic end to modify cysteine side-chains introduced into the intracellular and central parts of TM1 [56, 57], TM5 [60], TM6 [52, 53], TM11 [59] and TM12 [54, 55] (Fig. 4a, d).

The binding of organic anion open channel blockers within the inner vestibule is predominantly dependent on the presence of a single positive charge—that of K95 in TM1 (Fig. 4a, d). Neutralization of this positive charge causes a large decrease in the blocking potency of a broad range of different open channel blocking anions [46, 63], which suggests that a diverse range of negatively charged molecules can bind within the inner vestibule by interacting electrostatically with this pore-lining positive charge [25]. Manipulating the positive charge at this position also strongly affects the ability of lyotropic permeant anions to block Cl^- permeation [26], suggesting that this positive charge also contributes to a binding site in the inner vestibule for permeant anions, probably including Cl^- itself [23].

Recently neutralization of this key positive charge has also been shown to disrupt the normal lyotropic anion conductance selectivity sequence [23]. Whereas the relative conductance of small anions is predominantly determined by anion hydration energy in wild-type CFTR (Fig. 1f), all these anions showed very similar conductances in K95Q-CFTR [23]. Analysis of the effects of neutralization of the positive charge at K95 on anion binding and anion relative conductance was used to suggest that the strength of anion binding to a permeant anion binding site involving or close to K95 followed a lyotropic sequence—in other words, anions that are more easily dehydrated bind to this site more strongly than do anions that are more difficult to dehydrate—and that the relative strength of binding to this site then determines the relative conductance of different anions [23]. This suggestion would appear to confirm the long-standing hypothesis that lyotropic anion conductance sequence of CFTR (Fig. 1f) is a reflection of lyotropic anion binding to the pore—that tight binding of lyotropic anions results in longer residence time within the pore and consequently lower conductance. The finding that mutagenesis of K95 could disrupt the anion conductance selectivity sequence without strongly affecting anion permeability selectivity—whereas a mutation at the narrow region of the pore (F337A) strongly altered the anion permeability selectivity process with negligible effects on anion conductance selectivity—was also used to suggest that the pore effectively has two "selectivity filters" operating in series, an anion permeability selectivity filter at the narrow region and an anion conductance selectivity filter located within the inner vestibule [23].

Mutations that remove the positive charge at position 95 also greatly reduce single channel conductance by 80–90 % [62, 63], demonstrating an important role for this positive charge in the normal Cl^- conduction mechanism. While this was originally ascribed to an electrostatic role for this positive charge in attracting Cl^- ions to the pore [46, 63], more recent work has emphasized the importance of K95 in contributing to Cl^- ion binding inside the pore [23, 26]. While tight ion binding inside the pore might not be expected to result in high conductance—as seen in the lyotropic nature of anion relative conductance described above, in which tighter ion binding results in lower conductance—the presence of an anion binding site inside the inner vestibule might be required to maximize anion occupancy of the pore, which might in turn result in higher conductance. However, the relationship between anion occupancy of the pore and anion conductance has not been investigated in detail, and as such the exact role of K95 in maintaining high Cl^- conductance is not entirely understood.

While the positive charge of K95 appears essential for blocker binding in the inner vestibule, mutagenesis studies suggest that other side-chains in the inner vestibule also likely make contact with bound blocker molecules [89, 93]. Interestingly, the blocker binding properties of wild-type, as well as its single channel conductance, can be restored (following neutralization of K95) by second-site mutations that "move" the positive charge from K95 to other sites within the inner vestibule, in TM6 (I344K, V345K, M348K) [91] or TM12 (S1141K) [63]. Even wild-type anion conductance selectivity properties that are disrupted in K95Q are restored in K95Q/I344K, indicating that a positive charge in either TM1 or TM6 can fulfil the role of the putative anion conductance selectivity filter [23]. These results suggest that the presence of a positive charge within the inner vestibule, rather than its exact location at position 95, is required for the anion binding properties of wild-type CFTR [91]. However, it was noted that K95 appears to be the optimal position to locate this positive charge to maximize Cl^- conductance [91]. Furthermore, it appears that one is the optimal number of positive charges lining this region of the inner vestibule to support anion binding and Cl^- conductance. Thus, mutations that introduce a second positive charge at sites that can support anion binding (I344K, V345K, M348K, S1141K) do not lead to an increase in Cl^- conductance above wild-type levels [63, 91] or to altered anion conductance selectivity [23]. However, these mutations with an extra positive charge exhibit tighter anion binding within the inner vestibule [26, 63, 91], especially for multivalent anions [27, 51, 63, 91]. In fact, this strengthened anion binding has been shown to be detrimental to overall channel function, leading to reduced channel conductance at hyperpolarized voltages due to enhanced channel block by endogenous cytoplasmic anions [63, 73].

Mutation of uncharged amino acid side-chains lining the inner vestibule, in TM5 (F310, F311), TM6 (I344, V345, M348, A349) and TM12 (S1141, W1145, N1148), has little or no effect on Cl^- conductance [52, 54, 60, 63, 91, 93, 96], which, together with the charge-dependent effects of mutations involving K95 on Cl^- permeation [46, 63, 91] is consistent with the important interactions between the inner vestibule and permeating anions being of an electrostatic nature.

At the intracellular end of TM6 is another positive charge, R352, that has been suggested to interact electrostatically with Cl^- ions [64]. Seemingly consistent with this role, a cysteine side-chain substituted at this position is accessible to cytoplasmically applied MTS reagents [52, 53]. However, it has also been shown that R352 can form a salt bridge with negatively charged D993 in TM9 when the channel is open [78, 97, 98].

The ability to "transplant" the functionally important positive charge from K95 in TM1 to TM6 (I344, V345, M348) or TM12 (S1141) suggests that these pore-lining side-chains might be located close together in the three-dimensional architecture of the inner vestibule [63, 91] (Fig. 4d). Indeed, it was shown that a disulfide bond could be formed between cysteine side-chains substituted for K95 and I344 [56] as well as K95 and S1141 [63], constraining the relative proximity of these residues from different TMs. Metal bridges formed by Cd^{2+} ions have also been used to demonstrate close proximity between K95 and S1141; between S1141 and TM6 side-chains I344, V345 and M348; and between M348 and TM12 side-chains Q1144, W1145, V1147 and N1148 [50].

Many sites within the inner vestibule are accessible to large intracellular MTS reagents both in open and in closed channels [53–56, 60, 99], suggesting that this region is open to the cytoplasm throughout the gating cycle. Nevertheless, a number of different changes in the structure of the inner vestibule have been suggested to occur during channel opening and closing. Based on state-dependent changes in the accessibility of cysteine side-chains introduced into TM6 and TM12, it was suggested that these TM α-helices may undergo helical rotations of up to 100° during opening and closing [52, 54]. However, it has also been suggested that these state-dependent accessibility changes could reflect changes in interactions between different TMs rather than rotation of individual TMs [43]. State-dependent formation of Cd^{2+} bridges between cysteine side-chains suggested that TM6 and TM12 move apart when the channel opens, whereas TM1 and TM12 move closer together during opening [50]. While this study did not rule out either rotational or translational movement of these TMs during opening and closing, it did suggest that lateral separation and convergence of different TMs is the key conformational change that is required for the channel to open and close, since Cd^{2+} bridges that held TM6 and TM12 together stabilized the closed state of the channel, whereas a bridge that held TM1 together with TM12 stabilized the open state [50].

Anion attraction by the cytoplasmic pathway

Positively charged side-chains in the ICLs electrostatically attract cytoplasmic Cl^- ions to the internal entrance to the pore (Fig. 4a, e). Mutations and MTS modifications cause a charge-dependent effect on single channel Cl^- conductance at K190 (cytoplasmic extension to TM3), R248 (extension to TM4), R303 (extension to TM5), K370 (extension to TM6), and, to a lesser extent, K1041 and R1048 (extension to TM10) [47]. SCAM of additional residues with neutral side-chains in these TM extensions identified further parts of the cytoplasmic pathway [48]. At these sites within the cytoplasmic extensions to TMs 3, 4, 5 and 6, cysteine substitutions themselves had no effect on Cl^- conductance, however, modification with a negatively charged MTS reagent caused a reduction in Cl^- conductance, suggesting that the cytoplasmic pathway attracts Cl^- ions to the pore in an electrostatic fashion [48]. These results were used to suggest that Cl^- ions first enter the permeation pathway from the cytoplasm via a portal between the extensions to TMs 4 and 6, approximately at the level of K370 in the extension to TM6 [47, 48]. After entering the pore, Cl^- ions were then proposed to pass along a pathway formed by different parts of these TM extensions, into the inner vestibule formed by the intracellular ends of the TMs (Fig. 4e).

Beyond this role in electrostatic attraction of cytoplasmic Cl^- ions, little is known about the properties of the cytoplasmic pathway. Large, polyvalent suramin anions have been shown to block the open channel by electrostatic interaction with R303 at the extreme cytoplasmic end of TM5 [100], suggesting the location of a second anionic blocker binding site at a more superficial location into the pore from its cytoplasmic end than that involving K95 (see above). Unlike channel block involving interaction with K95, block by cytoplasmic suramin is independent of membrane potential, in spite of the suramin molecule carrying a net charge of −6, suggesting that its binding site involving R303 might be located outside of the membrane electric field [25, 100]. Interaction with R303 within the cytoplasmic pathway might also be involved in the inhibitory effects of other substances on CFTR, for example arachidonic acid [101]. Currently there is a lack of experimental evidence concerning the three-dimensional structure of the cytoplasmic pathway, and a lack of evidence for significant changes in its conformation during channel opening and closing. Molecular modeling studies have hinted that there may exist more than one (potentially

up to four) portal or entrance leading from the cytoplasm into the cytoplasmic pathway [42, 43]. However, since introduction of a negative charge (by MTS modification) at position 370, close to the mouth of the putative portal illustrated in Fig. 4e, reduced single channel Cl^- conductance by >75 %, it was proposed that most permeating Cl^- ions must use this entrance to access the channel pore [47, 48].

Integration of pore function

The structural and functional characterization of the pore summarized in Fig. 4 defines four seemingly distinct pore regions and their roles in anion attraction, binding, selectivity, and conductance. How do these regions of the pore act together to fulfil CFTR's role in the rapid conduction of Cl^-, HCO_3^- and other small anions across the cell membrane? Simply summing together the roles of the regions described in the preceding sections might suggest that the outer and inner vestibules, together with the cytoplasmic pathway, attract anions electrostatically toward the narrow region, where non-electrostatic interactions with uncharged amino acid side chains determine anion conductance and selectivity. However, there is experimental evidence that different parts of the pore interact with each other to determine overall pore function, and that this integration of function may be crucial to the normal anion permeation mechanism.

One commonly observed manifestation of this interaction between pore regions is the ability of anions bound to different sites in the pore to interact with one another. As described above, many different intracellular anions can block the pore by binding within the inner vestibule, probably by interacting with the positive charge of K95 [25]. In many cases block by intracellular anions is weakened by extracellular Cl^- [25] or other small monovalent anions [27, 102]. A recent detailed quantitative analysis of the interaction between an intracellular blocking anion [$Pt(NO_2)_4^{2-}$] and different extracellular anions suggested that two anions bind concurrently to sites in the inner vestibule (interacting with K95) and in the outer vestibule (interacting with R334) in a mutually antagonistic fashion [27]. However, the ways in which anions in these different regions of the pore are able to sense one another's presence—either by direct electrostatic interaction or by a propagated conformational change in the channel protein—are not currently known.

Antagonistic interactions between anions bound to different sites inside the pore may also have important implications for the mechanism of rapid Cl^- permeation. Mutations that remove the positive charge at either K95 [62, 63] or R334 [65, 76] are associated with reduced Cl^- conductance. At R334, the effect of different mutations on conductance was correlated with their ability to disrupt interactions between external Cl^- and internal anions [76]. Furthermore, it has been shown that the movement of two different permeant anions [$Au(CN)_2^-$ and Cl^-] in the pore is "coupled" rather than independent [102]. It has been suggested that interactions between concurrently bound Cl^- ions is necessary to destabilize Cl^- binding and ensure rapid Cl^- exit from the pore, resulting in maximization of the rate of Cl^- conductance [27, 35]. This model would be consistent with the established "multi-ion" mechanism of ion permeation in highly selective cation channel pores [85, 103, 104]. However, as described above, whether the interaction between Cl^- ions is direct or indirect is not yet established.

Conclusions from architecture to mechanism

As an ion channel, CFTR must form a continuous aqueous pathway for the movement of ions from the cytoplasm to the extracellular solution in its open state. Interactions between these substrate ions and pore-lining amino acids must then determine the observable functional properties of the channel such as its conductance, selectivity, ion binding properties, and blocker sensitivity, that are summarized in Fig. 1.

The overall shape of the Cl^- permeation pathway is now defined based on functional analysis and molecular modeling (Figs. 3, 4). This pathway appears to deviate somewhat from the central substrate translocation pathway expected for pseudosymmetrical ABC proteins [4], as well as from the central pore classically associated with most classes of ion channels. At its cytoplasmic end, Cl^- ions are now thought to enter the pore not centrally but via one or more lateral portals formed between the long ICLs (Figs. 2d, 3c, e, f, 4a, e) [42, 43, 47, 48]. This may allow Cl^- entry into the pore from the cytoplasm to occur relatively independently of conformational rearrangements occurring at the MSD:NBD boundary during NBD-driven channel gating. Active transporter ABC proteins are thought to transport substrate across the membrane by transitioning between "inward facing" and "outward facing" conformations of the MSDs, this transition being driven by ATP action at the NBDs [3, 4]. In the inward facing conformation, the inner ends of the MSDs are, therefore, expected to be separated, potentially allowing large substrate molecules to enter the cytoplasmic end of the transport pathway centrally [4]. The proposed ability of Cl^- ions to enter the permeation pathway via a lateral portal could, therefore, allow these ions to "short-circuit" this conformational change and enter the pore in both inward-facing and outward-facing conformations. Consistent with this model, it has been shown that even large

MTS molecules can enter the pore from the cytoplasm and penetrate as far as the inner vestibule both in the open state and in the closed state [53–56], in other words, presumably during any conformation of the MSDs visited during the gating cycle. Alternatively, it may be that CFTR exists in a permanent pseudo-outward-facing conformation with the MSDs sealed at their cytoplasmic ends, perhaps consistent with a single extracellular gate controlled by the NBDs [83, 95]. In either of these speculative scenarios, the existence of the lateral portal(s) would appear to represent a crucial step in the evolution of CFTR from an active transporter to an ion channel.

Once inside the permeation pathway, it appears that Cl^- ions continue to follow an off-centre route as the pass through the pore (Figs. 3c, f, 4). Functionally speaking, the pore is dominated by TM6, with somewhat supporting roles being played by TMs 1, 11 and 12 (summarized in Fig. 4). It is strikingly apparent from Fig. 3f that important pore-lining positive charges in TMs 1 and 6 are oriented approximately above the lateral portal from the cytoplasm (at least in this representation of the channel), allowing for the speculation that permeating Cl^- ions follow a fairly straight (if not central) pathway through the membrane that brings them into closest contact with these two important TMs.

Investigation of the physical basis of pore properties using structure–function analysis—again as summarized in Fig. 4—supports a somewhat simple model of Cl^- permeation (Fig. 5). The permeation pathway is decorated by fixed positive charges (provided by arginine and lysine side-chains) that attract Cl^- ions electrostatically, resulting in high substrate availability that is a prerequisite for high conductance. At least some of these positive charges (K95, and perhaps R334) contribute to binding sites for anions, probably including permeating Cl^- ions. The strength of ion binding to one site (in the inner vestibule, and including K95) dominates the residence time inside the pore for different anions, generating the observed lyotropic anion conductance sequence (Fig. 1f) and also resulting in susceptibility to open channel block by anions that bind tightly to this site. Once inside the pore, Cl^- ions are funneled towards a short, narrow uncharged region. The relatively restricted dimensions of this part of the pore mean that permeating ions approach closely to the pore walls, resulting in anion size selectivity (due to steric factors; Fig. 1d) and lyotropic anion permeability selectivity (likely due to small differences in anion:water and anion:pore interaction energies; Fig. 1e) and generating a relatively high resistance to anion permeation. Biophysical analyses also suggest that anions bound to different sites interact with each other, which may be another factor that acts to maximize the rate of Cl^- permeation through the pore (Fig. 5b). Similar anion selectivity and anion binding properties observed across multiple anion channel types [20, 31–36] might suggest that, in spite of their structural diversity, a similarly simple anion permeation mechanism to that outlined in Fig. 5 could be a common feature of these anion-transporting proteins.

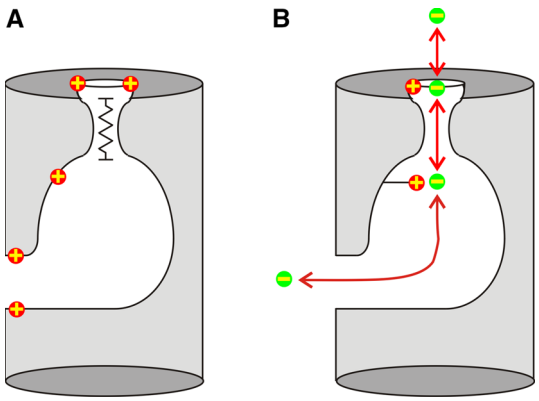

Fig. 5 Cartoon summary of current ideas concerning the functional architecture of the CFTR pore. **a** The narrow pore region represents a relatively high resistance, uncharged region of the pore. Chloride ions are attracted electrostatically towards this narrow region by fixed positive charges in the outer vestibule, inner vestibule, and cytoplasmic pathway. **b** Cl^- ions (*green balls*) are attracted towards binding sites in the inner vestibule (including K95) and outer vestibule (likely including R334). Chloride ions bound at these sites then interact antagonistically, weakening binding and ensuring rapid exit of bound ions from the pore

References

1. Riordan JR, Rommens JM, Kerem B, Alon N, Rozmahel R, Grzelczak Z, Zielenski J, Lok S, Plavsic N, Chou J-L, Drumm ML, Iannuzzi MC, Collins FS, Tsui L-C (1989) Identification of the cystic fibrosis gene: cloning and characterization of complementary DNA. Science 245:1066–1073
2. Dean M, Rzhetsky A, Alikmets R (2001) The human ATP-binding cassette (ABC) transporter superfamily. Genome Res 11:1156–1166
3. Rees DC, Johnson E, Lewinson O (2009) ABC transporters: the power to change. Nat Rev Mol Cell Biol 10:218–227
4. ter Beek J, Guskov A, Slotboom DJ (2014) Structural diversity of ABC transporters. J Gen Physiol 143:419–435
5. Gadsby DC, Vergani P, Csanády L (2006) The ABC protein turned chloride channel whose failure causes cystic fibrosis. Nature 440:477–483
6. Miller PS, Aricescu AR (2014) Crystal structure of a human $GABA_A$ receptor. Nature 512:270–275
7. Du J, Lü W, Wu S, Cheng Y, Gouaux E (2015) Glycine receptor mechanism elucidated by electron cryo-microscopy. Nature 526:224–229
8. Huang X, Chen H, Michelsen K, Schneider S, Shaffer PL (2015) Crystal structure of human glycine receptor-α3 bound to antagonist strychnine. Nature 526:277–280
9. Accardi A (2015) Structure and gating of CLC channels and exchangers. J Physiol 593:4129–4138

10. Pedemonte N, Galietta LJV (2014) Structure and function of TMEM16 proteins (anoctamins). Physiol Rev 94:419–459
11. Kane Dickson V, Pedi L, Long SB (2014) Structure and insights into the function of a Ca^{2+}-activated Cl^- channel. Nature 516:213–218
12. Jentsch TJ, Lutter D, Planells-Cases R, Ullrich F, Voss FK (2016) VRAC: molecular identification as LRRC8 heteromers with differential functions. Pflügers Arch 468:385–393
13. Frizzell RA, Hanrahan JW (2012) Physiology of epithelial chloride and fluid secretion. Cold Spring Harb Perspect Med 2:a009563
14. Jih K-Y, Hwang T-C (2012) Nonequilibrium gating of CFTR on an equilibrium theme. Physiology 27:351–361
15. Chong PA, Kota P, Dokholyan NV, Forman-Kay JD (2013) Dynamics intrinsic to cystic fibrosis transmembrane conductance regulator function and stability. Cold Spring Harb Perspect Med 3:a009522
16. Hwang T-C, Kirk KL (2013) The CFTR ion channel: gating, regulation, and anion permeation. Cold Spring Harb Perspect Med 3:a009498
17. Linsdell P, Hanrahan JW (1998) Adenosine triphosphate-dependent asymmetry of anion permeation in the cystic fibrosis transmembrane conductance regulator chloride channel. J Gen Physiol 111:601–614
18. McCarty NA, Zhang Z-R (2001) Identification of a region of strong discrimination in the pore of CFTR. Am J Physiol 281:L852–L867
19. Tabcharani JA, Linsdell P, Hanrahan JW (1997) Halide permeation in wild-type and mutant cystic fibrosis transmembrane conductance regulator chloride channels. J Gen Physiol 110:341–354
20. Smith SS, Steinle ED, Meyerhoff ME, Dawson DC (1999) Cystic fibrosis transmembrane conductance regulator. Physical basis for lyotropic anion selectivity patterns. J Gen Physiol 114:799–818
21. Linsdell P, Evagelidis A, Hanrahan JW (2000) Molecular determinants of anion selectivity in the cystic fibrosis transmembrane conductance regulator chloride channel pore. Biophys J 78:2973–2982
22. Linsdell P (2014) Functional architecture of the CFTR chloride channel. Mol Membr Biol 31:1–16
23. Linsdell P (2016) Anion conductance selectivity mechanism of the CFTR chloride channel. Biochim Biophys Acta 1858:740–747
24. Linsdell P (2001) Relationship between anion binding and anion permeability revealed by mutagenesis within the cystic fibrosis transmembrane conductance regulator chloride channel pore. J Physiol 531:51–66
25. Linsdell P (2014) Cystic fibrosis transmembrane conductance regulator chloride channel blockers: pharmacological, biophysical and physiological relevance. World J Biol Chem 5:26–39
26. Rubaiy HN, Linsdell P (2015) Location of a permeant anion binding site in the cystic fibrosis transmembrane conductance regulator chloride channel pore. J Physiol Sci 65:233–241
27. Linsdell P (2015) Interactions between permeant and blocking anions inside the CFTR chloride channel pore. Biochim Biophys Acta 1848:1573–1590
28. Muanprasat C, Sonawane ND, Salinas D, Taddei A, Galietta LJV, Verkman AS (2004) Discovery of glycine hydrazide pore-occluding CFTR inhibitors: mechanism, structure-activity analysis, and in vivo efficacy. J Gen Physiol 124:125–137
29. Zhou J-J, Fatehi M, Linsdell P (2007) Direct and indirect effects of mutations at the outer mouth of the CFTR chloride channel pore. J Membr Biol 216:129–142
30. Zhou J-J, Fatehi M, Linsdell P (2008) Identification of positive charges situated at the outer mouth of the CFTR chloride channel pore. Pflügers Arch 457:351–360
31. Bormann J, Hamill OP, Sakmann B (1987) Mechanism of anion permeation through channels gated by glycine and γ-aminobutyric acid in mouse cultured spinal neurones. J Physiol 385:243–286
32. Fahlke C (2001) Ion permeation and selectivity in ClC-type chloride channels. Am J Physiol 280:F748–F757
33. Machaca K, Qu Z, Kuruma A, Hartzell HC, McCarty NA (2002) The endogenous calcium-activated Cl channel in *Xenopus* oocytes: a physiologically and biophysically rich model system. Curr Top Membr 53:3–39
34. Hartzell C, Putzier I, Arreola J (2005) Calcium-activated chloride channels. Annu Rev Physiol 67:719–758
35. Linsdell P (2006) Mechanism of chloride permeation in the cystic fibrosis transmembrane conductance regulator chloride channel. Exp Physiol 91:123–129
36. Reyes JP, López-Rodríguez A, Espino-Saldaña AE, Huanosta-Gutiérrez A, Miledi R, Martínez-Torres A (2014) Anion permeation in calcium-activated chloride channels formed by TMEM16A from *Xenopus tropicalis*. Pflügers Arch 466:1769–1777
37. Rosenberg MF, O'Ryan LP, Hughes G, Zhao Z, Aleksandrov LA, Riordan JR, Ford RC (2011) The cystic fibrosis transmembrane conductance regulator (CFTR). Three-dimensional structure and localization of a channel gate. J Biol Chem 286:42647–42654
38. Hunt JF, Wang C, Ford RC (2013) Cystic fibrosis transmembrane conductance regulator (ABCC7) structure. Cold Spring Harb Perspect Med 3:a009514
39. Choudhury HG, Tong Z, Mathavan I, Li Y, Iwata S, Zirah S, Rebuffat S, van Veen HW, Beis K (2014) Structure of an antibacterial peptide ATP-binding cassette transporter in a novel outward occluded state. Proc Natl Acad Sci USA 111:9145–9150
40. Lee JY, Yang JG, Zhitnitsky D, Lewinson O, Rees DC (2014) Structural basis for heavy metal detoxification by an Atm1-type ABC exporter. Science 343:1133–1136
41. Kim J, Wu S, Tomasiak TM, Mergel C, Winter MB, Stiller SB, Robles-Colmanares Y, Stroud RM, Tampé R, Craik CS, Cheng Y (2015) Subnanometre-resolution electron cryomicroscopy structure of a heterodimeric ABC exporter. Nature 517:396–400
42. Mornon J-P, Hoffmann B, Jonic S, Lehn P, Callebaut I (2015) Full-open and closed CFTR channels, with lateral tunnels from the cytoplasm and an alternative position of the F508 region, as revealed by molecular dynamics. Cell Mol Life Sci 72:1377–1403
43. Corradi V, Vergani P, Tieleman DP (2015) Cystic fibrosis transmembrane conductance regulator (CFTR): closed and open state channel models. J Biol Chem 290:22891–22906
44. Linsdell P, Hanrahan JW (1996) Disulphonic stilbene block of cystic fibrosis transmembrane conductance regulator Cl^- channels expressed in a mammalian cell line and its regulation by a critical pore residue. J Physiol 496:687–693
45. Sheppard DN, Robinson KA (1997) Mechanism of glibenclamide inhibition of cystic fibrosis transmembrane conductance regulator Cl^- channels expressed in a murine cell line. J Physiol 503:333–346
46. Linsdell P (2005) Location of a common inhibitor binding site in the cytoplasmic vestibule of the cystic fibrosis transmembrane conductance regulator chloride channel pore. J Biol Chem 280:8945–8950
47. El Hiani Y, Linsdell P (2015) Functional architecture of the cytoplasmic entrance to the cystic fibrosis transmembrane conductance regulator chloride channel pore. J Biol Chem 290:15855–15865
48. El Hiani Y, Negoda A, Linsdell P (2016) Cytoplasmic pathway followed by chloride ions to enter the CFTR channel pore. Cell Mol Life Sci 73:1917–1925

49. El Hiani Y, Linsdell P (2014) Conformational changes opening and closing the CFTR chloride channel: insights from cysteine scanning mutagenesis. Biochem Cell Biol 92:481–488
50. El Hiani Y, Linsdell P (2014) Metal bridges illuminate transmembrane domain movements during gating of the cystic fibrosis transmembrane conductance regulator chloride channel. J Biol Chem 289:28149–28159
51. Linsdell P (2014) State-dependent blocker interactions with the CFTR chloride channel: implications for gating the pore. Pflügers Arch 466:2243–2255
52. Bai Y, Li M, Hwang T-C (2010) Dual roles of the sixth transmembrane segment of the CFTR chloride channel in gating and permeation. J Gen Physiol 136:293–309
53. El Hiani Y, Linsdell P (2010) Changes in accessibility of cytoplasmic substances to the pore associated with activation of the cystic fibrosis transmembrane conductance regulator chloride channel. J Biol Chem 285:32126–32140
54. Bai Y, Li M, Hwang T-C (2011) Structural basis for the channel function of a degraded ABC transporter, CFTR (ABCC7). J Gen Physiol 138:495–507
55. Qian F, El Hiani Y, Linsdell P (2011) Functional arrangement of the 12th transmembrane region in the CFTR chloride channel based on functional investigation of a cysteine-less variant. Pflügers Arch 462:559–571
56. Wang W, El Hiani Y, Linsdell P (2011) Alignment of transmembrane regions in the cystic fibrosis transmembrane conductance regulator chloride channel pore. J Gen Physiol 138:165–178
57. Gao X, Bai Y, Hwang T-C (2013) Cysteine scanning of CFTR's first transmembrane segment reveals its plausible roles in gating and permeation. Biophys J 104:786–797
58. Fatehi M, Linsdell P (2009) Novel residues lining the CFTR chloride channel pore identified by functional modification of introduced cysteines. J Membr Biol 228:151–164
59. Wang W, El Hiani Y, Rubaiy HN, Linsdell P (2014) Relative contribution of different transmembrane segments to the CFTR chloride channel pore. Pflügers Arch 466:477–490
60. Zhang J, Hwang T-C (2015) The fifth transmembrane segment of cystic fibrosis transmembrane conductance regulator contributes to its anion permeation pathway. Biochemistry 54:3839–3850
61. Gupta J, Evagelidis A, Hanrahan JW, Linsdell P (2001) Asymmetric structure of the cystic fibrosis transmembrane conductance regulator chloride channel pore suggested by mutagenesis of the twelfth transmembrane region. Biochemistry 40:6620–6627
62. Ge N, Muise CN, Gong X, Linsdell P (2004) Direct comparison of the functional roles played by different transmembrane regions in the cystic fibrosis transmembrane conductance regulator chloride channel pore. J Biol Chem 279:55283–55289
63. Zhou J-J, Li M-S, Qi J, Linsdell P (2010) Regulation of conductance by the number of fixed positive charges in the intracellular vestibule of the CFTR chloride channel pore. J Gen Physiol 135:229–245
64. St Aubin CN, Linsdell P (2006) Positive charges at the intracellular mouth of the pore regulate anion conduction in the CFTR chloride channel. J Gen Physiol 128:535–545
65. Smith SS, Liu X, Zhang Z-R, Sun F, Kriewall TE, McCarty NA, Dawson DC (2001) CFTR: covalent and noncovalent modification suggests a role for fixed charges in anion conduction. J Gen Physiol 118:407–431
66. Broadbent SD, Wang W, Linsdell P (2014) Interaction between two extracellular loops influences the activity of the cystic fibrosis transmembrane conductance regulator chloride channel. Biochem Cell Biol 92:390–396
67. Cui G, Rahman KS, Infield DT, Kuang C, Prince CZ, McCarty NA (2014) Three charged amino acids in extracellular loop 1 are involved in maintaining the outer pore architecture of CFTR. J Gen Physiol 144:159–179
68. Hämmerle MM, Aleksandrov AA, Riordan JR (2001) Disease-associated mutations in the extracytoplasmic loops of cystic fibrosis transmembrane conductance regulator do not impede biosynthetic processing but impair chloride channel stability. J Biol Chem 276:14848–14854
69. Infield DT, Cui G, Kuang C, McCarty NA (2016) Positioning of extracellular loop 1 affects pore gating of the cystic fibrosis transmembrane conductance regulator. Am J Physiol 310:L403–L414
70. Li M-S, Cowley EA, Linsdell P (2012) Pseudohalide anions reveal a novel extracellular site for potentiators to increase CFTR function. Br J Pharmacol 167:1062–1075
71. Broadbent SD, Ramjeesingh M, Bear CE, Argent BE, Linsdell P, Gray MA (2015) The cystic fibrosis transmembrane conductance regulator is an extracellular chloride sensor. Pflügers Arch 467:1783–1794
72. Wright AM, Gong X, Verdon B, Linsdell P, Mehta A, Riordan JR, Argent BE, Gray MA (2004) Novel regulation of CFTR channel gating by external chloride. J Biol Chem 279:41658–41663
73. Li M-S, Holstead RG, Wang W, Linsdell P (2011) Regulation of CFTR chloride channel macroscopic conductance by extracellular bicarbonate. Am J Physiol 300:C65–C74
74. Zhou J-J, Linsdell P (2009) Evidence that extracellular anions interact with a site outside the CFTR chloride channel pore to modify channel properties. Can J Physiol Pharmacol 87:387–395
75. Beck EJ, Yang Y, Yaemsiri S, Raghuram V (2008) Conformational changes in a pore-lining helix coupled to cystic fibrosis transmembrane conductance regulator channel gating. J Biol Chem 283:4957–4966
76. Gong X, Linsdell P (2004) Maximization of the rate of chloride conduction in the CFTR channel pore by ion-ion interactions. Arch Biochem Biophys 426:78–82
77. Gong X, Linsdell P (2003) Molecular determinants and role of an anion binding site in the external mouth of the CFTR chloride channel pore. J Physiol 549:387–397
78. Rahman KS, Cui G, Harvey SC, McCarty NA (2013) Modeling the conformational changes underlying channel opening in CFTR. PLoS One 8:e74574
79. Wang W, Linsdell P (2012) Relative movements of transmembrane regions at the outer mouth of the cystic fibrosis transmembrane conductance regulator channel pore during channel gating. J Biol Chem 287:32136–32146
80. Linsdell P (2015) Metal bridges to probe membrane ion channel structure and function. Biomol Concepts 6:191–203
81. Zhang Z-R, Song B, McCarty NA (2005) State-dependent chemical reactivity of an engineered cysteine reveals conformational changes in the outer vestibule of the cystic fibrosis transmembrane conductance regulator. J Biol Chem 280:41997–42003
82. Wang W, Linsdell P (2012) Alternating access to the transmembrane domain of the ATP-binding cassette protein cystic fibrosis transmembrane conductance regulator (ABCC7). J Biol Chem 287:10156–10165
83. Gao X, Hwang T-C (2015) Localizing a gate in CFTR. Proc Natl Acad Sci USA 112:2461–2466
84. Linsdell P, Tabcharani JA, Rommens JM, Hou Y-X, Chang X-B, Tsui L-C, Riordan JR, Hanrahan JW (1997) Permeability of wild-type and mutant cystic fibrosis transmembrane conductance regulator chloride channels to polyatomic anions. J Gen Physiol 110:355–364

85. Hille B (2001) Ion channels of excitable membranes. Sinauer, Sunderland
86. Gouaux E, MacKinnon R (2005) Principles of selective ion transport in channels and pumps. Science 310:1461–1465
87. Linsdell P, Zheng S-X, Hanrahan JW (1998) Non-pore lining amino acid side chains influence anion selectivity of the human CFTR Cl^- channel expressed in mammalian cell lines. J Physiol 512:1–16
88. Gupta J, Linsdell P (2003) Extent of the selectivity filter region in the CFTR chloride channel. Mol Membr Biol 20:45–52
89. McDonough S, Davidson N, Lester HA, McCarty NA (1994) Novel pore-lining residues in CFTR that govern permeation and open-channel block. Neuron 13:623–634
90. Fatehi M, St. Aubin CN, Linsdell P (2007) On the origin of asymmetric interactions between permeant anions and the CFTR chloride channel pore. Biophys J 92:1241–1253
91. El Hiani Y, Linsdell P (2012) Tuning of CFTR chloride channel function by location of positive charges within the pore. Biophys J 103:1719–1726
92. Sheppard DN, Travis SM, Ishihara H, Welsh MJ (1996) Contribution of proline residues in the membrane-spanning domains of cystic fibrosis transmembrane conductance regulator to chloride channel function. J Biol Chem 271:14995–15001
93. Cui G, Song B, Turki HW, McCarty NA (2012) Differential contribution of TM6 and TM12 to the pore of CFTR identified by three sulfonylurea-based blockers. Pflügers Arch 463:405–418
94. Gao X, Hwang T-C (2016) Spatial positioning of CFTR's pore-lining residues affirms an asymmetrical contribution of transmembrane segments to the anion permeation pathway. J Gen Physiol 147:407–422
95. Wei S, Roessler BC, Icyuz M, Chauvet S, Tao B, Hartman JL, Kirk KL (2016) Long-range coupling between the extracellular gates and the intracellular ATP binding domains of multidrug resistance protein pumps and cystic fibrosis transmembrane conductance regulator channels. FASEB J 30:1247–1262
96. Sorum B, Czégé D, Csanády L (2015) Timing of CFTR pore opening and structure of its transition state. Cell 163:724–733
97. Cui G, Zhang Z-R, O'Brien AR, Song B, McCarty NA (2008) Mutations at arginine 352 alter the pore architecture of CFTR. J Membr Biol 222:91–106
98. Jordan IK, Kota KC, Cui G, Thompson CH, McCarty NA (2008) Evolutionary and functional divergence between the cystic fibrosis transmembrane conductance regulator and related ATP-binding cassette transporters. Proc Natl Acad Sci USA 105:18865–18870
99. Wang W, Linsdell P (2012) Conformational change opening the CFTR chloride channel pore coupled to ATP-dependent gating. Biochim Biophys Acta 1818:851–860
100. St Aubin CN, Zhou J-J, Linsdell P (2007) Identification of a second blocker binding site at the cytoplasmic mouth of the cystic fibrosis transmembrane conductance regulator chloride channel pore. Mol Pharmacol 71:1360–1368
101. Zhou J-J, Linsdell P (2007) Molecular mechanism of arachidonic acid inhibition of the CFTR chloride channel. Eur J Pharmacol 563:88–91
102. Gong X, Linsdell P (2003) Coupled movement of permeant and blocking ions in the CFTR chloride channel pore. J Physiol 549:375–385
103. Sather WA, McCleskey EW (2003) Permeation and selectivity in calcium channels. Annu Rev Physiol 65:133–159
104. Roux B (2005) Ion conduction and selectivity in K^+ channels. Annu Rev Biophys Biomol Struct 34:153–171
105. Zhang Z-R, Zeltwanger S, McCarty NA (2000) Direct comparison of NPPB and DPC as probes of CFTR expressed in *Xenopus* oocytes. J Membr Biol 175:35–52